[10] C. Tellambura, A. Annamalai, and V. K. Bhargava, "Unified analysis of switched diversity systems in independent and correlated fading channels," *IEEE Trans. Commun.*, vol. 49, no. 11, pp. 1955–1965, Nov. 2001.
[11] G. Femenias, "Reference-based dual switched and stay diversity systems over correlated Nakagami fading channels," *IEEE Trans. Veh. Technol.*, vol. 52, no. 4, pp. 902–918, Jul. 2003.
[12] L. Xiao and X. Dong, "New results on the BER of switched diversity combining over Nakagami fading channels," *IEEE Commun. Lett.*, vol. 9, no. 2, pp. 136–138, Feb. 2005.
[13] N. Maleki, E. Karami, and M. Shiva, "Optimization of antenna array structures in mobile handsets," *IEEE Trans. Veh. Technol.*, vol. 54, no. 4, pp. 1346–1351, Jul. 2005.
[14] S. Wei, D. Goeckel, and R. Janaswamy, "On the capacity of MIMO systems with antenna arrays of fixed volume," *IEEE Trans. Wireless Commun.*, vol. 4, no. 4, pp. 1608–1621, Jul. 2005.
[15] C. C. Tan and N. C. Beaulieu, "Infinite series representations of the bivariate Rayleigh and Nakagami-m distributions," *IEEE Trans. Commun.*, vol. 45, no. 10, pp. 1159–1161, Oct. 1997.
[16] Q. T. Zhang, "Maximal-ratio combining over Nakagami fading channels with an arbitrary branch covariance matrix," *IEEE Trans. Veh. Technol.*, vol. 48, no. 4, pp. 1141–1150, Jul. 1999.
[17] R. K. Mallik, "On multivariate Rayleigh and exponential distributions," *IEEE Trans. Inf. Theory*, vol. 49, no. 6, pp. 1499–1515, Jun. 2003.
[18] G. K. Karagiannidis, D. A. Zogas, and S. A. Kotsopoulos, "On the multivariate Nakagami-m distribution with exponential correlation," *IEEE Trans. Commun.*, vol. 51, no. 8, pp. 1240–1244, Aug. 2003.
[19] G. K. Karagiannidis, D. A. Zogas, and S. A. Kotsopoulos, "An efficient approach to multivariate Nakagami-m distribution using Green's matrix approximation," *IEEE Trans. Wireless Commun.*, vol. 2, no. 5, pp. 883–889, Sep. 2003.
[20] Y. Chen and C. Tellambura, "Performance analysis of three-branch selection combining over arbitrarily correlated Rayleigh-fading channels," *IEEE Trans. Wireless Commun.*, vol. 4, no. 3, pp. 861–865, May 2005.
[21] Y. Chen and C. Tellambura, "Infinite series representation of the trivariate and quadrivariate Rayleigh distribution and their applications," *IEEE Trans. Commun.*, vol. 53, no. 12, pp. 2092–2101, Dec. 2005.
[22] P. Dharmawansa, N. Rajatheva, and C. Tellambura, "Infinite series representations of the trivariate and quadrivariate Nakagami-m distributions," *IEEE Trans. Wireless Commun.*, vol. 6, no. 12, pp. 4320–4328, Dec. 2007.
[23] P. S. Bithas and P. T. Mathiopoulos, "Performance analysis of SSC diversity receivers over correlated Ricean fading satellite channels," *EURASIP J. Wireless Commun. Netw.*, vol. 2007, no. 1, Jan. 2007, Art. ID 25361, 9 p.
[24] P. S. Bithas, N. C. Sagias, and P. T. Mathiopoulos, "Dual diversity over correlated Ricean fading channels," *J. Commun. Netw.*, vol. 9, no. 1, pp. 67–74, Mar. 2007.
[25] G. C. Alexandropoulos, N. C. Sagias, F. I. Lazarakis, and K. Berberidis, "New results for the multivariate Nakagami-m fading model with arbitrary correlation matrix and applications," *IEEE Trans. Wireless Commun.*, vol. 8, no. 1, pp. 245–255, Jan. 2009.
[26] J. Reig, "Multivariate Nakagami-m distribution with constant correlation model," *Int. J. Electron Commun. (AEU)*, vol. 63, no. 1, pp. 46–51, Jan. 2009.
[27] K. Peppas and N. C. Sagias, "A trivariate Nakagami-m distribution with arbitrary covariance matrix and applications to generalized selection diversity receivers," *IEEE Trans. Commun.*, vol. 57, no. 7, pp. 1896–1902, Jul. 2009.
[28] G. C. Alexandropoulos, "Performance analysis of multichannel receivers over correlated fading channels," Ph.D. dissertation, Univ. Patras, Patras, Greece, Jun. 2010, to be published.
[29] I. S. Gradshteyn and I. M. Ryzhik, *Table of Integrals, Series, and Products,* 6th ed. New York: Academic, 2000.
[30] A. S. Krishnamoorthy and M. Parthasarathy, "A multivariate gamma-type distribution," *Ann. Math. Statist.*, vol. 22, no. 4, pp. 549–557, Dec. 1951.
[31] D. B. Owen, "A table of normal integrals," *Commun. Statist.-Simul. Comput.*, vol. 9, no. 4, pp. 389–419, Oct. 1980.

A Hybrid Architecture for Delay Analysis of Interleaved FEC on Mobile Platforms

Kyungtae Kang, *Member, IEEE*, Cheolgi Kim, *Member, IEEE*, and Kyung-Joon Park, *Member, IEEE*

***Abstract*—Forward error correction (FEC) is the preferred way of coping with the error-prone nature of wireless links in broadcasting systems, because it can provide a bounded delay, which is a particular consideration for real-time multimedia applications. Additionally, controlling the variability of the delay, or jitter, is important in achieving seamless multimedia services. We show that error control using Reed–Solomon (RS) FEC in the medium-access control (MAC) layer can be a major source of jitter. We predict the expected delay incurred by RS decoding for varying levels of block interleaving in a mobile, under a range of channel conditions, using a hybrid simulation and analytic approach, which is based on the error statistics of data transmission over fading channels. The results allow us to determine the size of the buffer required to avoid frequent service interruptions.**

***Index Terms*—Delay estimation, hybrid architecture, interleaved forward error correction (FEC), mobile systems.**

I. Introduction

Broadcast and multicast services in CDMA2000 wireless networks [1], [2] can simultaneously provide uniform high-quality multimedia to a large number of subscribers. For this purpose, an outer forward error-correction (FEC) code in the medium-access control (MAC) layer is used in combination with the physical-layer inner turbo code [3]. This combination enhances the transmission efficiency, irrespective of any explicit power control. The CDMA2000 air specification [4] states that Reed–Solomon (RS) codes with the coding rates of 12/16, 13/16, and 14/16 should be considered as the options for the outer code, owing to their superior performance at low error rates [5]–[7].

An RS code is specified by a tuple (N, K), where K and $(N - K)$ are the number of information bytes and parity bytes, respectively, in each codeword. The RS algebraic erasure decoding procedure is then able to correct up to $(N - K)$ damaged bytes, which are located by a cyclic redundancy check in the physical layer, in each RS codeword. The physical-layer protocol erases these damaged bytes and informs the RS erasure decoder of their locations.

Before applying RS encoding, the access network transfers the data, which consists of broadcast security packets [4], into a buffer called an error control block (ECB) for each logical channel. The data are entered into the ECB row by row, RS coding is applied to the columns of the ECB, and the access network transmits the data from the ECB on the broadcast channel, again by row. Each row of an ECB constructs M broadcast MAC packets, and each of these packets contains 125 B of the ECB as its payload, together with a 2-bit MAC trailer. The

Manuscript received June 24, 2009; revised September 30, 2009. First published January 15, 2010; current version published May 14, 2010. This work was supported by the Korean Government Ministry of Education and Human Resources Development under Korea Research Foundation Grant KRF-2007-357-D00174. The review of this paper was coordinated by Prof. C. P. Oestges.

The authors are with the Thomas M. Siebel Center for Computer Science, Department of Computer Science, University of Illinois at Urbana-Champaign, Urbana, IL 61801-2302 USA (e-mail: ktkang@illinois.edu; cheolgi@illinois.edu; kjp@illinois.edu).

Color versions of one or more of the figures in this paper are available online at http://ieeexplore.ieee.org.

Digital Object Identifier 10.1109/TVT.2010.2040640

purpose of the ECB is to permit block interleaving [10], [11], which allows efficient recovery from the bursts of errors, which frequently occur in communicating with mobile subscribers. The extent of this block interleaving can be adjusted by varying the value of M, which is the width of the ECB. A wide ECB provides increased time diversity, which improves the performance, even in the presence of time-varying shadowing.

Kang *et al.* [12] investigated this error-recovery structure within the context of data transmission in broadcast and multicast services in CDMA2000 wireless networks. They analyzed the RS decoding process in detail, derived a simplified model of the time that it requires, and presented the results of experiments performed with the SNU Energy Explorer (SEE) [13], which is a web-based mobile platform testbed based on the ARM7TDMI processor. Using this timing model, Cho *et al.* [12] estimated the time taken by RS decoding with a Gilbert–Elliot [13], [14] channel model of Rayleigh fading and found that jitter in the processing time of the RS decoder can lead to a discontinuity in multimedia streaming. Their evaluation of the jitter bound allowed them to suggest a system architecture based on a jitter earliest due date [15] model, which can ensure the continuity of real-time services for multimedia applications over a third-generation cellular broadcast network. However, this analysis only considered the maximum amount of interleaving when the ECB was wide enough to perfectly randomize the channel errors under most channel conditions. Additionally, the Gilbert–Elliot model has a limited capacity to represent the combination of long error bursts with a highly variable error rate, although it precisely describes the long-term error rate [16].

In this paper, we complement earlier work by considering various levels of block interleaving. We have developed a stochastic analysis of delay that allows the formulation of a delay model of RS decoding to accommodate various levels of ECB interleaving and conditions of the fading channel. Furthermore, we have replaced the bit-level Gilbert–Elliot model with a more sophisticated block-level error model of the fading channel to improve the accuracy of our analysis. In this model, the Markov approximation is combined with a detailed threshold model to provide a closer description of the block-error process that takes place in fading channels. These structures support hybrid analysis, in which the packet error rate (PER) of the physical channel is first obtained by simulating the inner code, and then, the PER is used to derive the parameters of the Markov model. This enables us to analyze the delay involved in MAC-layer RS decoding across the layers by taking the physical layer into account. Later, in this paper, we will establish the validity of this hybrid approach by comparing its results with those obtained by brute-force simulation. Our overall aim is to provide an integrated framework and, thus, to promote insights that can materially affect the design of the developing protocols that are necessary in each service layer of a wireless network if the goal of high-quality multimedia broadcast systems is to be achieved.

To the best of our knowledge, this study is the first analysis of the timing aspect of RS decoding in the context of broadcast services in CDMA2000 wireless networks. It is intended to provide a foundation for high-quality broadcast services, with special emphasis on delay-sensitive applications, such as multimedia. We have focused on CDMA2000 networks in this study, because they are currently deployed in many countries, but the applicability of the proposed hybrid analytic architecture is not limited to those networks, because it is both modular and extensible. Different protocol designs can easily be plugged into the architecture, allowing the performance of newer systems such as third-generation partnership project–long-term evaluation [17] or WiMAX [18] to be predicted and appropriate design parameters to be chosen.

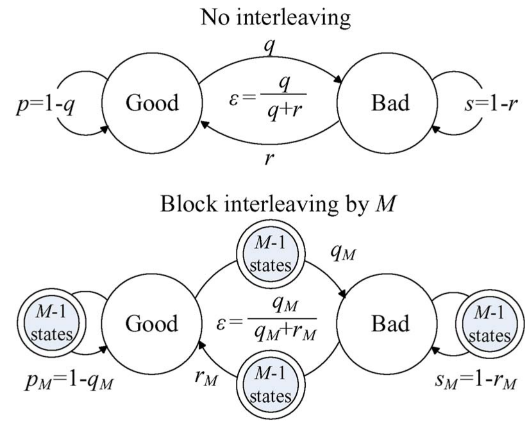

Fig. 1. Representation of the error process by a state diagram with Markov parameters.

II. Background and Related Work

A. Error Statistics in Data Transmission Over Fading Channels

Wireless channels with memory have widely been studied. However, some real-world channels do not lend themselves to theoretical analysis, and the development of simplified models is desirable. The investigation by Zorzi *et al.* [19] of the behavior of the block errors that arise in data transmission over fading channels took the specific coding and modulation scheme [19] into account and tracked the fading process symbol by symbol. This detailed approach includes the simulation of the third-order statistics of the block-error process. It was shown that a Markov approximation is a good model of the block-error process for a range of modulation schemes, block lengths, and error-correction capabilities of the outer code. Additionally, it was shown that the relationship between the marginal error rate and the transition probability essentially depends on an appropriately normalized version of the Doppler frequency. This relationship is, in fact, almost similar to that of the simple threshold model, which assumes that the value of the fading envelope is constant throughout the duration of a data block, and a block is successfully received if and only if the value of the fading envelope is above a certain threshold, for which closed-form expressions were obtained in [20], for the Rayleigh-fading case. This fact suggests a unified approach to the modeling of the physical channel, which could simplify the analysis of the upper layer protocols.

In this detailed threshold model [19], the Markov process is specified by two independent parameters q and r, which are the transition probabilities that relate the transmission status of the consecutive packets, as shown in Fig. 1. (Recall that each MAC packet contains a 125-B payload.) The channel generates a packet error whenever the Markov chain reaches the bad state, which results in the erasure of the payload that it contains. Finally, the analytical expression for the Markov parameters of the threshold model for flat Rayleigh fading [19] is

$$F = -\frac{1}{\log(1-\varepsilon)} \tag{1}$$

where F is the fading margin, and ε is the steady-state PER, which is given as follows:

$$\varepsilon = \frac{r}{q+r}. \tag{2}$$

The average length of a burst of packet errors is $1/r$, where

$$r = \frac{Q\left(\sqrt{\frac{2/F}{1-\rho^2}}, \rho\sqrt{\frac{2/F}{1-\rho^2}}\right) - Q\left(\rho\sqrt{\frac{2/F}{1-\rho^2}}, \sqrt{\frac{2/F}{1-\rho^2}}\right)}{e^{\frac{1}{F}}-1}. \tag{3}$$

The term ρ is the correlation coefficient of the two samples of the complex Gaussian fading process and is equal to $\rho = J_0(2\pi f'_D)$, where $J_0(\cdot)$ is the Bessel function of the first kind and of zeroth order, and (f'_D) is the normalized version of the Doppler frequency. In particular, the value of f'_D is calculated as $f'_D = f_D N_{\mathrm{BL}} T$, where f_D is the maximum Doppler frequency, N_{BL} is the block size, and T is the symbol duration. When the value of f'_D is very small, the fading process is highly autocorrelated (slow fading); on the other hand, for very large values of f'_D, the two samples of the channel are almost independent (fast fading). Additionally

$$Q(x, y) = \int_y^\infty e^{-\frac{x^2+w^2}{2}} I_0(xw) w \, dw \tag{4}$$

is the Marcum-Q [21] function. Thus, the relationship between the two parameters ε and r can be expressed as

$$r = \frac{1-\varepsilon}{\varepsilon} \left[Q(\theta, \rho\theta) - Q(\rho\theta, \theta)\right] \tag{5}$$

where

$$\theta = \sqrt{\frac{-2\log(1-\varepsilon)}{1-\rho^2}}. \tag{6}$$

Equation (5) can be used as an approximation for the functional relationship between the Markov parameters and the average PER. This Markov approximation takes the average PER and the speed of a fading process as the input parameters and is used in conjunction with the detailed threshold model to describe the behavior of the block-error process produced by a fading channel. It is a useful tool to simplify the performance evaluation of higher layer protocols.

The preliminary step to use this approximation is, therefore, to determine the inputs of the threshold model, which are the average PER ε and normalized version of the Doppler frequency (f'_D). In particular, the average PER depends on the details of the modulation/coding scheme used and the physical-layer packet sizes. By considering the signal-to-noise ratio (SNR) of the forward data channel, types of modulations, code rate, and the physical-layer packet size, the average PER experienced by the mobile is obtained using the coded modulation library (CML) from the Iterative Solutions [22], which is an open-source library for simulating turbo codes in MATLAB. The CML contains support for block turbo codes while supporting various modulation formats, as well as channel types such as additive white Gaussian noise and block Rayleigh fading. It even incorporates the CDMA2000 turbo code, which makes the simulation of CDMA2000 turbo encoding and decoding very straightforward.

B. Measuring the Execution Time of RS Decoding

RS decoding can be carried out with either the software or special-purpose hardware. The major difficulty in software implementations is that general-purpose processors do not support Galois field arithmetic; however, their advantage is that there is no need for special hardware. In addition, software implementation of the RS decoder allows the legacy systems to be relatively easily upgraded by changing their firmware. Recent improvements in the RS algorithms, together with the increases in the processor performance, indicate that software implementations can now run at relatively high data rates.

We used a software implementation of the RS erasure decoder, which is highly optimized for speed, memory, and platform, particularly with respect to the Berlekamp algorithm [23]. An optimized version of the Berlekamp algorithm called Berlekamp–Massey [24] is an efficient way of finding the shortest linear feedback shift register (LFSR) for a given output sequence. A slightly modified Berlekamp–Massey algorithm, which solves the equivalent problem of obtaining the smallest polynomial that describes a linearly recurrent sequence, has recently been suggested [25]. A sample implementation provided by Henry Minsky [26] and managed by the SourceForge software development and revision control system was used in our experiments.

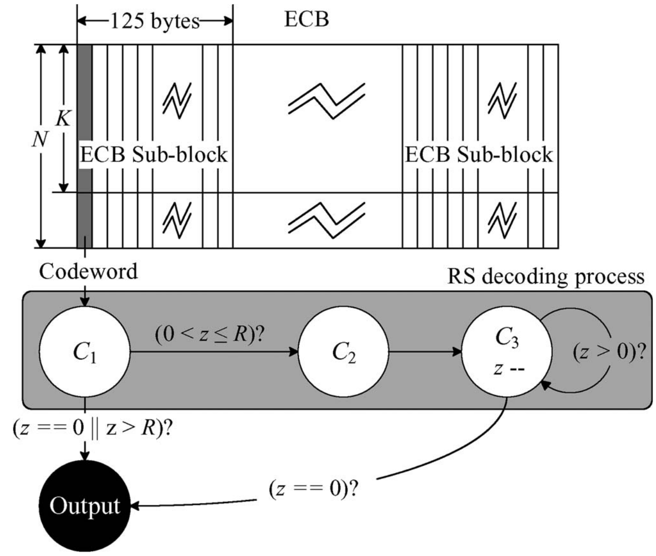

Fig. 2. Computational components C_1, C_2, and C_3 of the RS decoding process.

Previously [12], we analyzed the RS decoding process in detail and derived a simplified model of the time that it requires. In our model, the process is split into three computational components, as shown in Fig. 2: C_1 computes the syndrome of a received codeword to determine whether there are any erasures at all and then decides whether to try to correct them; if erasures are present, C_2 builds the syndromes needed to correct them, and C_3 performs the loops required to make the corrections. Thus, C_1 operates on every codeword received, C_2 is called once for each codeword that contains erasures, and C_3 is repeatedly invoked until no more erasures remain in that codeword.

An ECB subblock is a group of 125 codewords, and $T_{\mathrm{sb}}^{(N,K)}(z)$ is the time required to decode an ECB subblock that has been encoded with an (N, K) code, when that subblock contains z packet erasures. If the value of z is larger than 0 or less than or equal to $(N-K)$, then the total processing time can be determined as follows [12]:

$$T_{\mathrm{sb}}^{(N,K)}(z) = T_1^{(N,K)} + T_2^{(N,K)} + zT_3^{(N,K)} \tag{7}$$

where $T_i^{(N,K)}$ is the time taken by the ith component to decode an ECB subblock containing a single packet erasure. However, if the value of z is zero or larger than $(N-K)$, then $T_{\mathrm{sb}}^{(N,K)}(z)$ is equal to $T_1^{(N,K)}$. Values of $T_i^{(N,K)}$ were experimentally measured using the SEE and are presented in Table I.

III. Analytic Model of the Relationship Between Delay and Block Interleaving

Fig. 1 shows that the amount of block interleaving also affects the Markov description of consecutive packets in an ECB subblock. With M-block interleaving, there are M possible transitions of the "channel state" that can take place between two consecutive packets within a particular ECB subblock, because the threshold model that we previously outlined assumes that the fading process remains constant

TABLE I
TIME TAKEN BY EACH COMPUTATIONAL COMPONENT TO DECODE AN ECB SUBBLOCK CONTAINING A SINGLE PACKET ERASURE

RS code	$T_i^{(N,K)}$		
(N,K)	$T_1^{(N,K)}$	$T_2^{(N,K)}$	$T_3^{(N,K)}$
(16,12)	1487.5	102937.5	6850.0
(16,13)	1012.5	82325.0	6537.5
(16,14)	537.5	62737.5	6137.5
(32,24)	7612.5	194925.0	8287.5
(32,26)	5637.5	147375.0	7500.0
(32,28)	3687.5	103525.0	6712.5

(μs)

for the duration of one packet. A binary Markov process for the threshold model is shown [19] to be an adequate approximation for Doppler speeds between about 1 and 70 m/s. On the basis that we are considering speeds within this range, the resulting Markov transition parameters (q_M, r_M) can be determined from the following relation:

$$\begin{pmatrix} 1-q_M & r_M \\ q_M & 1-r_M \end{pmatrix} \triangleq \begin{pmatrix} 1-q & r \\ q & 1-r \end{pmatrix}^M. \tag{8}$$

Subsequently, to utilize the timing model (7) and the results obtained from it, as described in the previous section, we need to estimate how many erasures each ECB subblock can contain. By assuming that each ECB subblock consists of N packets, we can determine the probability of the mth ECB subblock $(1 \le m \le M)$ containing z erasures in N packets, depending on the channel condition Φ, which is represented by the tuple (ε, f'_D), as well as on the transmission status of the first packet in that ECB, which is represented by Ψ (can be (G)ood or (B)ad), as follows:

$$P^N(m,z|\Phi,\Psi) = P_G^N(m,z|\Phi,\Psi) + P_B^N(m,z|\Phi,\Psi) \tag{9}$$

where $P_G^N(m,z|\Phi,\Psi)$ and $P_B^N(m,z|\Phi,\Psi)$ represent the probability that the mth ECB subblock contains z erasures in N packets when the transmission of the Nth packet in that subblock is successful or corrupted, respectively, indicating that the events are mutually exclusive. These two probabilities are given as follows:

$$P_G^N(m,z|\Phi,\Psi) = \begin{cases} r_M P_B^{N-1}(m,z|\Phi,\Psi) \\ \quad +(1-q_M)P_G^{N-1}(m,z|\Phi,\Psi), & (0 \le z \le N-1) \\ 0, & (z=N) \end{cases} \tag{10}$$

$$P_B^N(m,z|\Phi,\Psi) = \begin{cases} (1-r_M)P_B^{N-1}(m,z-1|\Phi,\Psi) \\ \quad +q_M P_G^{N-1}(m,z-1|\Phi,\Psi), & (1 \le z \le N) \\ 0, & (z=0). \end{cases} \tag{11}$$

As it is obvious that the values of $P_G^N(m,N|\Phi,\Psi)$ and $P_B^N(m,0|\Phi,\Psi)$ are zero, we can obtain the probabilities that the mth ECB subblock, consisting of N packets, contains zero or N packet erasures (i.e., $z=0$ or N), depending on the transmission status of the first packet of the ECB Ψ as follows:

$$\begin{aligned} P^N(m,0|\Phi,\Psi) &= P_G^N(m,0|\Phi,\Psi) \\ &= P_G^1(m,0|\Phi,\Psi)(1-q_M)^{(N-1)} \end{aligned} \tag{12}$$

$$\begin{aligned} P^N(m,N|\Phi,\Psi) &= P_B^N(m,N|\Phi,\Psi) \\ &= P_B^1(m,1)(1-r_M)^{(N-1)}. \end{aligned} \tag{13}$$

When $1 \le z \le N-1$, the number of packet erasures within an ECB subblock can also be predicted using the functions derived from (10) and (11). Each of these functions is recursively executed, and eventually, an irreducible value is obtained, which is $P_G^j(m,j-1|\Phi,\Psi)$ for P_G and $P_B^k(m,1|\Phi,\Psi)$ for P_B. These expressions can be expanded as follows:

$$P_G^j(m,j-1|\Phi,\Psi) = P_B^1(m,1|\Phi,\Psi)(1-r_M)^{j-2}r_M \tag{14}$$

$$P_B^k(m,1|\Phi,\Psi) = P_G^1(m,0|\Phi,\Psi)(1-q_M)^{k-2}q_M \tag{15}$$

where $(2 \le j,k \le N)$. The terms $P_G^1(m,0|\Phi,\Psi)$ and $P_B^1(m,1|\Phi,\Psi)$ are the probabilities that delivery of the first packet in the mth $(m \ge 2)$ ECB subblock either succeeds or fails, respectively, and are equal to

$$P_G^1(m,0|\Phi,\Psi) = (1-q_m)P_G^1(1,0|\Phi,\Psi) + r_m P_B^1(1,1|\Phi,\Psi) \tag{16}$$

$$P_B^1(m,1|\Phi,\Psi) = q_m P_G^1(1,0|\Phi,\Psi) + (1-r_m)P_B^1(1,1|\Phi,\Psi) \tag{17}$$

where the initial variable $P_G^1(1,0|\Phi,\Psi)$ and $P_B^1(1,1|\Phi,\Psi)$ represent the probability of the transmission status of the first packet in that particular ECB as being *successful* or a *failure*, respectively. When the average PER is ε, the probability of successful delivery is $1-\varepsilon$ and $P_G^1(1,0|\Phi,G) = 1 - P_B^1(1,1|\Phi,G) = 1$, and the probability of failure is ε and $P_G^1(1,0|\Phi,B) = 1 - P_B^1(1,1|\Phi,B) = 0$. Finally, the probabilities that the mth $(1 \le m \le M)$ ECB subblock contains z packet erasures $P^N(m,z|\Phi)$ can be expressed in terms of the previously defined quantities, i.e.,

$$\begin{aligned} P^N(m,z|\Phi) &= P^N(\Phi,\Psi=G)P^N(m,z|\Phi,\Psi=G) \\ &\quad + P^N(\Phi,\Psi=B) \\ P^N(m,z|\Phi,\Psi=B) &= (1-\varepsilon)P^N(m,z|\Phi,\Psi=G) \\ &\quad + \varepsilon P^N(m,z|\Phi,\Psi=B). \end{aligned} \tag{18}$$

Thus, using (N,K) RS codes, the expected delay caused by RS decoding of an ECB under various channel conditions $E[\text{delay}|\varepsilon, f'_D, N, K, M]$ can be predicted using

$$E[\text{delay}|\varepsilon, f'_D, N, K, M] = \sum_{m=1}^{M}\sum_{z=0}^{N} T_{\text{sb}}^{(N,K)}(z)P^N(m,z|\Phi). \tag{19}$$

IV. EVALUATION OF THE RESULTS

It has been reported [4] that wireless coverage significantly shrinks, even when using a (32,24) RS code, as the data rate is raised from 614.4 to 1228.8 kb/s, for mobiles in both pedestrian and vehicular situations. We will therefore assume the use of quadrature phase-shift keying (QPSK) modulation and a data rate of 614.4 kb/s, for a forward broadcast channel encoded with a turbo code with a rate of one third. The modulation and data rate used in the forward traffic channel [27] determine the size of each physical-layer packet, which is 128 B $(N_{\text{BL}} = 128)$ for the modulation, coding, and data rate considered in our study.

We use a hybrid approach to analyze the delay incurred by RS decoding and consider the threshold model to give a good estimate of the Markov parameters p, q, r, and s for the broad range of the two system parameters PER and Doppler speed f'_D. We can obtain a PER by simulation using CML [22], which contains support for the CDMA2000 turbo code and a fading channel. From that PER, we can then derive the parameters of the Markov chain using the threshold model, which then form part of our model of the delay in MAC-layer

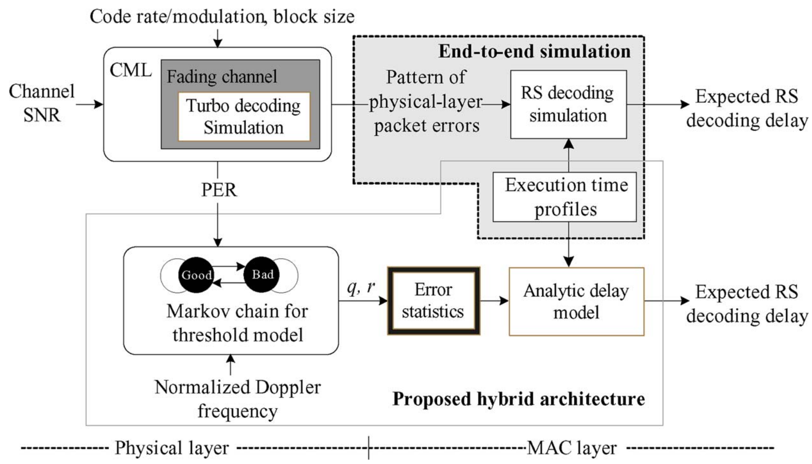

Fig. 3. Hybrid framework for analyzing the MAC-layer delay in mobile receivers.

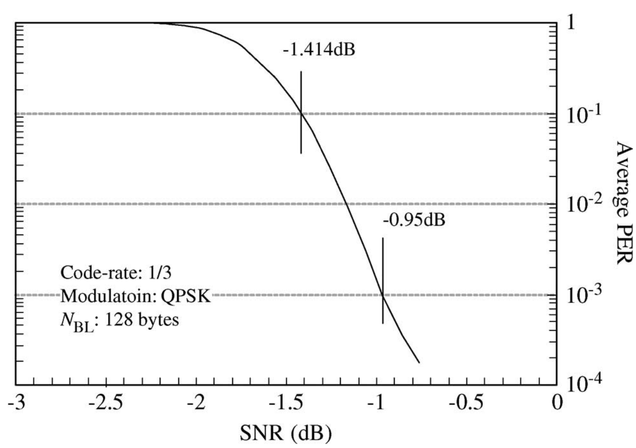

Fig. 4. Effect of turbo coding on the average PER for varying values of the SNR.

RS decoding, as shown in Fig. 3. We have also run fuller simulations using CML, in which we simulate both turbo and RS decoding, on top of the fading channel. We will compare the results obtained by these two approaches. The values of f'_D that we considered were 0.01 and 0.1, corresponding to speeds of about 2 m/s (slow fading) and 20 m/s (fast fading), respectively, with a carrier frequency of 900 MHz and a reference data rate of 614.4 kb/s [28]. Each packet received at the mobile is filled into the ECB in rows over a period of 1 s, and decoding is then carried out along the columns. All the codewords were encoded with the RS code (32,24). The value of M affects the level of block interleaving, and we tried values of 2, 4, 8, or 16.

Fig. 4 shows the average PER for different values of the SNR, when the inner code rate is one third and the physical-layer packet size is 1024 bits. These results, which were obtained from the CML turbo coding simulation, illustrate the performance of turbo coding in CDMA2000. Thus, for example, we can see that the resulting average PER varies between 0.001 and 0.1 as the value of the SNR for each QPSK symbol varies between -1.414 and -0.95 dB. The parameters of the Markov model when the SNR of the forward data channel is -1.414 or -0.95 dB and the values of f'_D are 0.01 or 0.1 can be found in Table II.

Fig. 5 shows values for the average delay incurred by RS decoding of a single ECB subblock, which illustrates the effect of block interleaving on delay. In Fig. 5, we compare the brute-force and the proposed hybrid methods to assess the accuracy of our approach. The discrepancy between the methods reaches 8% in the worst case, due to the shortcomings of the threshold model, which does not consider the

TABLE II
EXAMPLE PARAMETERS OF THE MARKOV MODEL

SNR	-1.414dB		-0.95dB	
ε	0.01		0.1	
f'_D	q	r	q	r
0.01	0.0006712	0.67055	0.0081277	0.07315
0.1	0.0009955	0.99457	0.0699767	0.62980

implications of a particular inner turbo code, and is limited to uncoded coherent phase-shift keying and noncoherent frequency-shift keying. Nevertheless, we are satisfied to an extent with the results obtained from the hybrid analytic method, which approximate those obtained by full end-to-end simulation reasonably well, as shown in Fig. 5. This shows that the performance of a turbo code can adequately be modeled by a threshold model that determines the chance of a block being successfully received by considering the value of the fading envelope to a given threshold. The adequacy of the model is more clearly shown in Fig. 4, in which we see that the PER drops from 1 to 0 in response to an increase in SNR of only 2 dB (from -2.5 dB to -0.5 dB).

The average delay incurred by RS decoding of an ECB subblock increases as the SNR drops to a threshold at which it is no longer possible to recover all the errors. If further errors occur, the RS decoder gives up on error correction, and the expected delay sharply drops. The slower one of our example mobiles with a smaller f'_D experiences longer error bursts with relatively long error-free intervals between them. Conversely, the mobile that is subject to faster fading experiences shorter but more frequent error bursts so that the errors are more sparsely distributed within the ECB for the same value of the SNR. As the second component C_2 of the RS decoder takes much longer to run than the other two computational components [12], the mere presence of errors has more effect on the delay than their number in an ECB. Thus, although the expected delay in the faster mobile is longer than that in the slower mobile (see Fig. 5), saturation eventually occurs in both mobiles for any given PER when the error bursts are sufficiently interleaved by a large value of M.

Additionally, the average delay is longer for larger values of M, because the probability that an ECB subblock contains any corrupted packets is higher if the ECB is larger. Conversely, when M is small, error bursts are concentrated into some ECB subblocks, whereas others that are transmitted under the same channel conditions contain no errors at all; as a result, the average delay incurred by RS decoding of a single ECB subblock decreases. However, this delay eventually saturates when the ECB becomes large enough to provide sufficient interleaving to completely counter the error bursts. This saturation point comes sooner for the faster mobile.

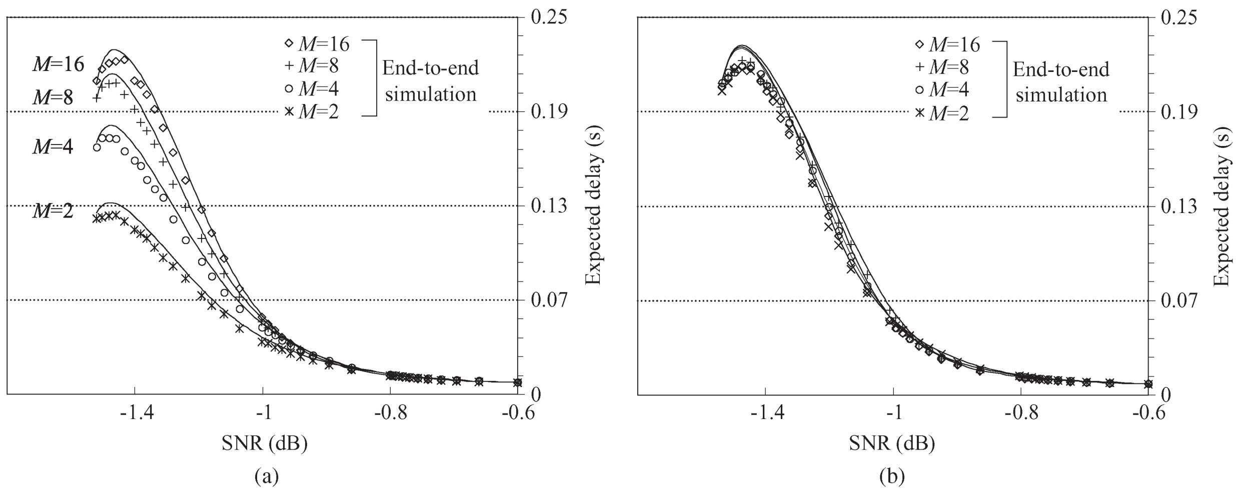

Fig. 5. Expected delay incurred in RS decoding of a single ECB subblock. (a) 2 m/s ($f'_D = 0.01$). (b) 20 m/s ($f'_D = 0.1$).

V. Conclusion

RS codes have been adopted as a method of FEC in the MAC layer for multimedia broadcasting in the CDMA2000 cellular network environment. We have evaluated the delay that RS decoding imposes on data transmission over a fading channel, taking into account the channel conditions that a mobile is likely to experience and the levels of block interleaving that are available. For this purpose, we have formulated a hybrid method and validated its accuracy. In this approach, a PER is obtained by simulation and then used to derive the parameters of the Markov model; finally, we were able to determine the average delay incurred by RS decoding, using an analytic model that we have developed. This method is extensible, because it has a modular architecture, allowing different designs of each module to be plugged in easily so that the expected performance of new wireless systems can be predicted.

Acknowledgment

The authors would like to thank the anonymous referees for providing valuable comments and suggestions that improved the quality of this paper.

References

[1] J. Wang, R. Sinnarajah, T. Chen, Y. Wei, and E. Tiedemann, "Broadcast and multicast services in CDMA2000," *IEEE Commun. Mag.*, vol. 42, no. 2, pp. 76–82, Feb. 2004.

[2] K. Kang, Y. Cho, J. Cho, and H. Shin, "Scheduling scalable multimedia streams for 3G cellular broadcast and multicast services," *IEEE Trans. Veh. Technol.*, vol. 56, no. 5, pp. 2655–2672, Sep. 2007.

[3] C. Berrou and A. Glavieux, "Near optimum error correcting coding and decoding: Turbo-codes," *IEEE Trans. Commun.*, vol. 44, no. 10, pp. 1261–1271, Oct. 1996.

[4] P. Agashe, R. Rezaiifar, and P. Bender, "CDMA2000 high rate broadcast packet data air interface design," *IEEE Commun. Mag.*, vol. 42, no. 2, pp. 83–89, Feb. 2004.

[5] W. J. Ebel and W. H. Tranter, "The performance of Reed-Solomon codes on a bursty-noise channel," *IEEE Trans. Commun.*, vol. 43, no. 2–4, pp. 298–306, Feb.–Apr. 1995.

[6] L. Rizzo, "On the feasibility of software FEC," Univ. Pisa, Pisa, Italy, DEIT Tech. Rep. LR-970131, Jan. 1997.

[7] G. C. Cardarilli, S. Pontarelli, M. Re, and A. Salsano, "Analysis of errors and erasures in parity sharing RS codecs," *IEEE Trans. Comput.*, vol. 56, no. 12, pp. 1721–1726, Dec. 2007.

[8] Y. Q. Shi, X. M. Zhang, Z.-C. Ni, and M. Ansari, "Interleaving for combating bursts of errors," *IEEE Circuits Syst. Mag.*, vol. 4, no. 1, pp. 29–42, First Quarter, 2004.

[9] K. Kang, "Probabilistic analysis of data interleaving for Reed-Solomon coding in BCMCS," *IEEE Trans. Wireless Commun.*, vol. 7, no. 10, pp. 3878–3888, Oct. 2004.

[10] K. Kang, Y. Cho, and H. Shin, "Energy-efficient MAC-layer error recovery for mobile multimedia applications in 3GPP2 BCMCS," *IEEE Trans. Broadcast.*, vol. 53, no. 1, pp. 338–349, Mar. 2007.

[11] I. Lee, Y. Choi, Y. Cho, Y. Joo, H. Lim, H. G. Lee, H. Shim, and N. Chang, "Web-based energy exploration tool for embedded systems," *IEEE Des. Test Comput.*, vol. 21, no. 6, pp. 572–586, Nov./Dec. 2004.

[12] Y. Cho, K. Kang, and H. Shin, "Seamless multimedia broadcasting over CDMA2000 BCMCS networks," in *Proc. IEEE ICC*, Jun. 2007, pp. 5628–5635.

[13] E. N. Gilbert, "Capacity of a burst-noise channel," *Bell Syst. Tech. J.*, vol. 39, pp. 1253–1266, Sep. 1960.

[14] M. Mushkin and I. Bar-David, "Capacity and coding for the Gilbert-Elliot channels," *IEEE Trans. Inf. Theory*, vol. 35, no. 6, pp. 1277–1290, Nov. 1989.

[15] D. C. Verma, H. Zhang, and D. Ferrari, "Delay jitter control for real-time communication in a packet switching network," in *Proc. IEEE TRICOMM*, Apr. 1991, pp. 35–46.

[16] K. V. Cardoso and J. F. Rezende, "Accurate hidden Markov modeling of packet losses in indoor 801.11 networks," *IEEE Commun. Lett.*, vol. 13, no. 6, pp. 417–419, Jun. 2009.

[17] E. Dahlman, S. Parkvall, J. Skold, and P. Beming, *3G Evolution, Second Edition: HSPA and LTE for Mobile Broadband*. New York: Academic, 2008.

[18] B. Li, Y. Qin, C. P. Low, and C. L. Gwee, "A survey on mobile WiMAX," *IEEE Commun. Mag.*, vol. 45, no. 12, pp. 70–75, Dec. 2007.

[19] M. Zorzi, R. R. Rao, and L. B. Milstein, "Error statistics in data transmission over fading channels," *IEEE Trans. Commun.*, vol. 46, no. 11, pp. 1468–1477, Nov. 1998.

[20] M. Zorzi and R. R. Rao, "ARQ error control on fading mobile radio channels," *IEEE Trans. Veh. Technol.*, vol. 46, no. 2, pp. 445–455, May 1997.

[21] J. G. Proakis, *Digital Communications*. New York: McGraw-Hill, 2008.

[22] Iterative Solutions. [Online]. Available: http://www.iterativesolutions.com

[23] E. R. Berlekamp, *Algebraic Coding Theory*. New York: McGraw-Hill, 1968.

[24] J. L. Massey, "Shift register synthesis and BCH decoding," *IEEE Trans. Inf. Theory*, vol. IT-15, no. 1, pp. 122–127, Jan. 1969.

[25] N. B. Atti, G. M. Diaz-Toca, and H. Lombardi, "The Berlekamp-Massey algorithm revisited," *Applicable Algebra Eng., Commun. Comput.*, vol. 17, no. 1, pp. 75–82, Apr. 2006.

[26] A Reed-Solomon Error-Correcting Encoder/Decoder Library Written in C. [Online]. Available: http://rscode.sourceforge.net

[27] P. Bender, P. Black, M. Grob, R. Padovani, N. Sindhushayana, and A. Viterbi, "CDMA/HDR: A bandwidth-efficient high-speed wireless data service for nomadic users," *IEEE Commun. Mag.*, vol. 38, no. 7, pp. 70–77, Jul. 2000.

[28] W. C. Jakes, *Microwave Mobile Communications*. New York: Wiley-IEEE Press, 1994.